Kovove Mater. 63 2025 69–77
DOI: 10.31577/km.2025.2.69

High-strength and high-conductivity bimetallic Fe/Cu wires

Justyna Domagała-Dubiel*, Wiesław Kazana, Krzysztof Marszowski, Joanna Kulasa

Łukasiewicz Research Network – Institute of Non-Ferrous Metals, Sowinskiego 5, Gliwice, Poland

Received 28 November 2024, received in revised form 25 February 2025, accepted 8 March 2025

Abstract

The article presents research results on the microstructure, mechanical and electrical properties of a newly developed Fe/Cu bimetallic wire characterized by high strength and electrical conductivity. The wire was obtained using the "rod-in-tube" technology, finally drawn to a diameter of 0.20 mm. Appropriate heat treatment was selected to obtain a wire with high strength properties. The microstructure of the wire after cold drawing was examined using an optical microscope (OM) and a scanning electron microscope (SEM) equipped with an EDS detector. Tests were performed to determine the mechanical and electrical properties. The appropriate heat treatment allows for the desired pearlitic microstructure of the steel core, which guarantees the high tensile strength of the bimetallic wire, approximately 2035 MPa, after the final drawing. The volume fraction of the copper layer ensures high electrical properties – approximately 50 % IACS.

K e y w o r d s: bimetallic wires, Fe/Cu composite wire, pearlitic microstructure, wire drawing, mechanical properties

1. Introduction

The dynamic development of industry places increasingly higher demands on materials that combine high mechanical properties and high electrical conductivity. Copper-coated steel wires have a wide range of applications, including in telecommunications, energy, electronics, automotive, defense, machinery and transport industries as a replacement for traditionally used copper wire. The reason is that the properties of these bimetallic wires combine the good strength of steel with the good conductivity and corrosion resistance of copper. Due to different material properties, producing a bimetallic wire, which is composed of different materials, poses greater difficulties than producing single-phase wires. Steel/copper clad wire has mechanical properties that neither single-phase nor steel wire can possess. Bimetallic copper-clad steel wires successfully replace pure copper wires and can be cheaper than single copper wires. The copper layer provides low electrical resistance, while the central steel core provides high structural strength, which can be achieved using high-carbon steel and appropriate heat treatment [1–3].

Currently, the main methods for preparing bimetallic wire with a copper layer are the welding and electroplating methods. Hot-dip coating, continuous extrusion, overlaying, and hot welding methods are also known [4]. The welding method is to gradually form a copper strip in a multi-roll arrangement into a slit tube on a steel core and longitudinally weld the Cu strip with argon shielding or other welding methods and connect copper and steel in the drawing process to form a copper-steel bimetallic wire [5]. A known method of obtaining Fe/Cu bimetallic wires by welding involves forming a tubular jacket on a steel core [6]. In this method, the strip is shaped into a slit tube on a mild steel core, where the slot is joined by TIG welding. Then the bimetallic wire is cold drawn, with inter-operative heat treatments. The tensile strength of the finished wire with a diameter of 0.4 mm is $Rm = 1050$ MPa, and the electrical conductivity is 19.5 MS m^{-1}. In the work [7], the subject of research was the microstructure of bimetallic wires made of low-carbon steel 1006 (LCSW) and high-carbon steel 1055 (HCSW). These wires were covered with a metal strip of oxygen-free copper (99.95 %). The copper strip was formed continuously on a steel rod. The litera-

*Corresponding author: e-mail address: justyna.domagala-dubiel@imn.lukasiewicz.gov.pl

Table 1. Chemical composition of steel C72D (wt.%)

C	Mn	Si	P	S	Cr	Ni	Cu	Fe
0.72	0.65	0.20	0.02	0.03	0.15	0.10	0.23	rest

ture also describes solutions for preparing an Fe/Cu bimetallic wire by electroplating [8]. The copper-clad steel wire is drawn to a smaller diameter. Annealing treatment is performed at 740–750 °C for 7–9 hours. Five drawing operations are performed using the presented method for producing copper-clad steel wires. High-strength wires with a nominal conductivity of up to 40 % IACS are known.

This article presents the test results of a newly developed Fe/Cu bimetallic wire using the rod-in-tube method with a final diameter of 0.20 mm, which provides high strength and conductivity of approximately 50 % IACS.

2. Experimental procedure

The initial materials for the tests included a C72D steel rod with a diameter of 8 mm and a Cu-ETP copper tube with an external diameter of ø 14.4 mm and a wall thickness of 1.7 mm. The chemical composition of C72D steel is shown in Table 1.

To select the appropriate tube wall thickness for the steel core, assuming a 50 % volume fraction of the steel core to the copper layer, for a known value of the steel core diameter (d_r) and volume fraction, the relationship for the tube wall thickness (g) can be derived:

$$4g^2 + 4d_r g - d_r^2 = 0, \tag{1}$$

hence for $d_r = 8$ mm and a volume fraction of 50 %, the wall thickness g is $1.6568 \sim 1.7$ mm.

After annealing at 650 °C for 3 hours, a C72D rod with a diameter of ø 8 mm, constituting the core of the wire, was placed in a copper tube with a diameter of ø 14.4 mm and a wall thickness of 1.7 mm. Before inserting the steel rod into the copper tube, the rod was mechanically cleaned, including surface activation. The inner part of the copper tube was also mechanically activated and degreased. The percentage of copper to high carbon steel was 50:50 by volume. In the next step, the copper pipe was tightened onto the steel rod by drawing to a diameter of 11 mm. After tightening, softening-diffusion annealing was carried out for 3 hours at 650 °C in a protective atmosphere. Then, the Fe/Cu semi-finished product was drawn with a total deformation of about 50 %, and heat treatments were carried out at 630 °C for 2.5 h for diameters of

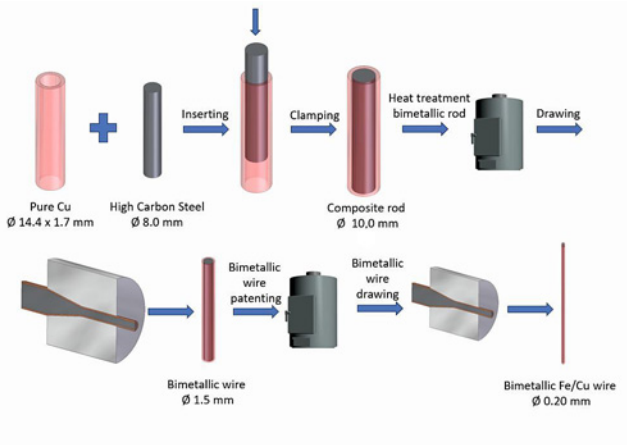

Fig. 1. Schematic view of the manufacturing process of the Fe/Cu bimetallic wire.

6.1, 4.2, 2.9, and 2.1 mm. Then the wire ø 2.1 mm was drawn to ø 1.5 mm in diameter. The wire prepared in this way was subjected to the patenting process at a temperature of 850 °C for 10 minutes and then cooled with compressed air for approximately 15 seconds. At the final stage, after the patenting process, the Fe/Cu wire was drawn to a final diameter of 0.20 mm without additional inter-operational heat treatment, with an average unit deformation of 12 %. Figure 1 shows a schematic view of the Fe/Cu bimetallic wire manufacturing process.

Metallographic tests were performed on wire samples embedded in thermohardening resins. After mounting, the samples were ground and then polished. The samples were etched to reveal the microstructure of the steel core.

Microstructural observations of the wires in cross-section were made using a light microscope and a LEO Gemini 1525 scanning electron microscope.

Qualitative X-ray microanalysis and analysis of the surface distribution of alloying elements in wire samples were performed on cross-sections on a scanning electron microscope with an EDS X-ray energy-dispersive spectrometer.

The microhardness of the steel core and copper layer in the cross-section of the bimetallic wire was determined using a microhardness tester, Future-Tech FM-700, at a load of 100 g for 15 s.

A static tensile test with determination of the tensile strength (TS) and elongation (E) was performed at room temperature using an Instron 4505/5500R universal testing machine, by the PN-EN ISO 6892-1: 2016 standard: Metals. Tensile test. Part 1: Method of test at room temperature. The tests were performed for three samples, and the arithmetic mean was calculated. The surfaces of selected fractures after the tensile test were examined using SEM.

The electrical resistivity was measured using a

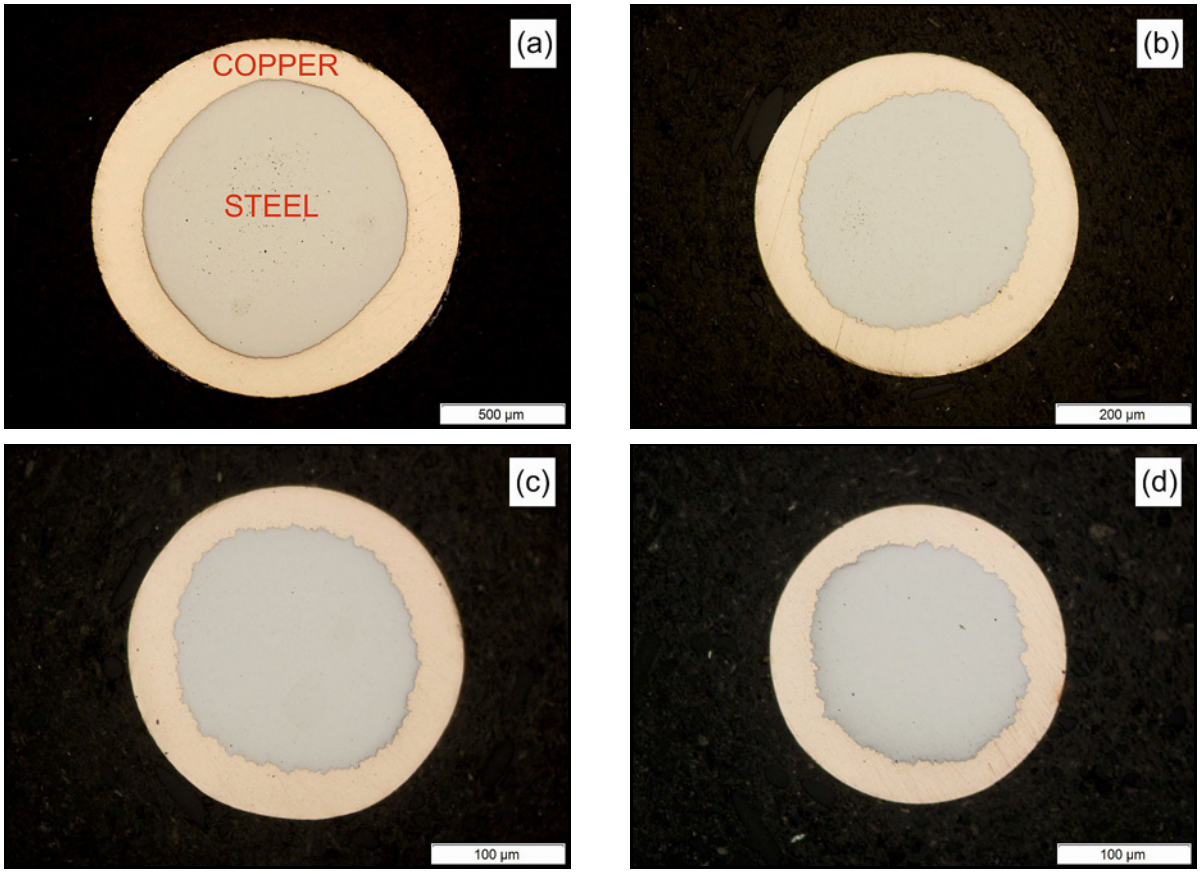

Fig. 2. The cross section of the Fe/Cu bimetalic wire after drawing; (a) ø 1.50 mm, mag. 75×, (b) ø 0.50 mm, mag. 200×, (c) ø 0.25 mm, mag. 400×, and (d) final bimetallic wire ø 0.20 mm, mag. 400×.

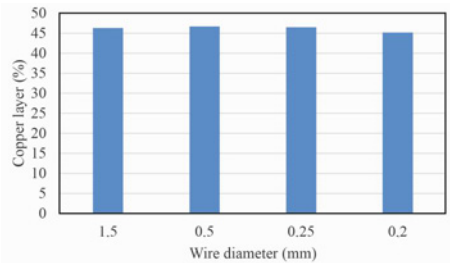

Fig. 3. Copper content depending on the diameter of the Fe/Cu wire.

technical method, using a measuring bench that enabled a separate connection of a power source and a millivoltmeter to the voltage terminals. An ammeter was connected in series with the power source to verify the current flowing through the circuit. Measurements were made at an ambient temperature of 20 °C.

3. Results and discussion

3.1. Microstructure characteristics

The cross-section of the Fe/Cu wire with a diameter of 1.50, 0.50, 0.25 mm, and the final one with a diameter of 0.20 mm is presented in Fig. 2. Based on the images shown, good quality of the bonding in the contact area of the steel core and copper layer was observed. No cracks or cavities were found between the layers. Based on the measurements of the inner diameter of the wire steel core and the outer diameter of the wire, the copper content was determined (Fig. 3). A constant copper content for the analysed wires was confirmed (46 % ± 1 %).

The elemental distribution of the copper layer and steel core was confirmed by elemental mapping in the SEM images on the cross-section of the Fe/Cu bimetallic wire (Fig. 4).

The microstructure of the steel core in the Fe/Cu bimetallic wire with a diameter of 1.50 mm after the patenting (AP) process is shown in Fig. 5. The patenting of the Fe/Cu wire with a diameter of 1.50 mm affects the microstructure remodelling of the steel core. Appropriate high-temperature treatment causes the formation of austenite in the steel. As a result of cooling, the resulting steel structure consists of very fine pearlite. As a rule, the carbon content of cold-drawn pearlitic steel wires is from 0.7 to 1.0 % by weight, and the amount of other additives is small; in partic-

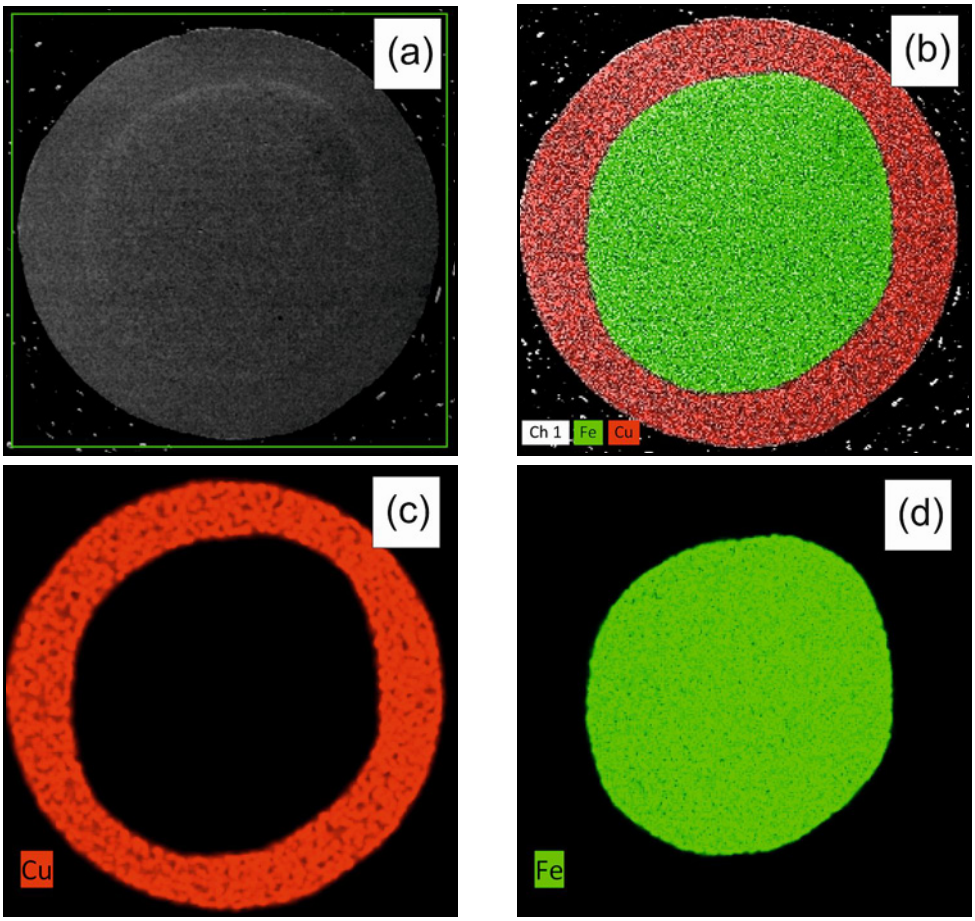

Fig. 4. Cross-sectional SEM image (a) and element mapping of (b)–(d) the Fe/Cu wire.

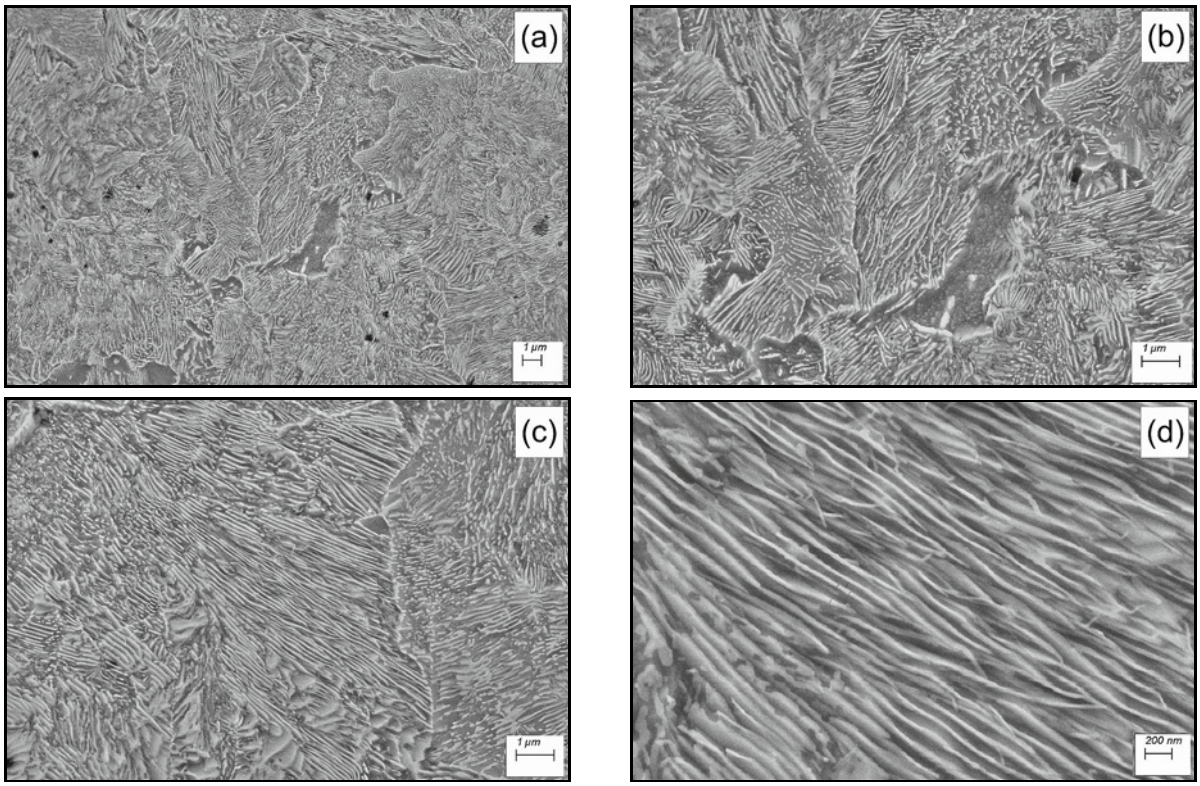

Fig. 5. Pearlitic structure at a normal cross-section of the 1.50 mm Fe/Cu wires drawn after patenting: (a) mag. 10,000×, (b) mag. 20,000×, (c) mag. 20,000×, and (d) mag. 70,000×, SEM.

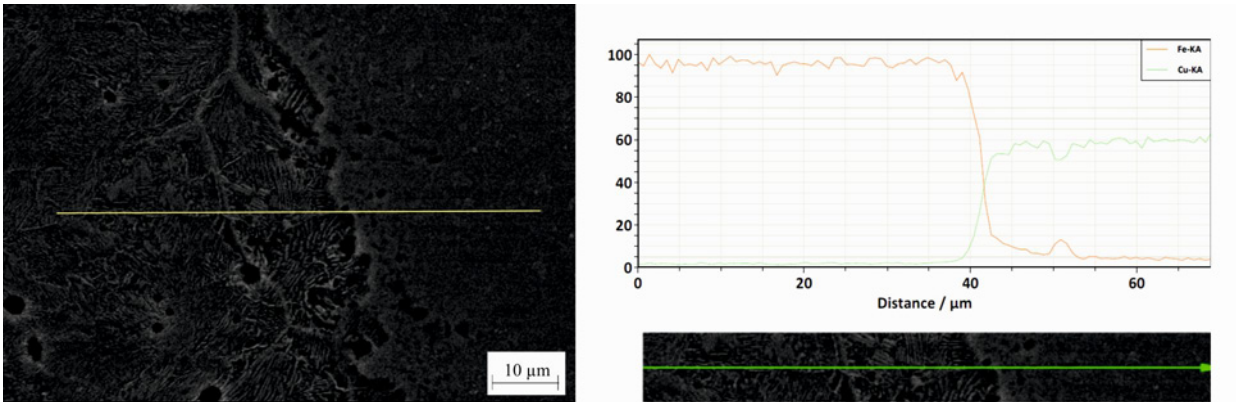

Fig. 6. Linear analysis of changes in the chemical composition of the Fe/Cu wire with a diameter of 1.50 mm.

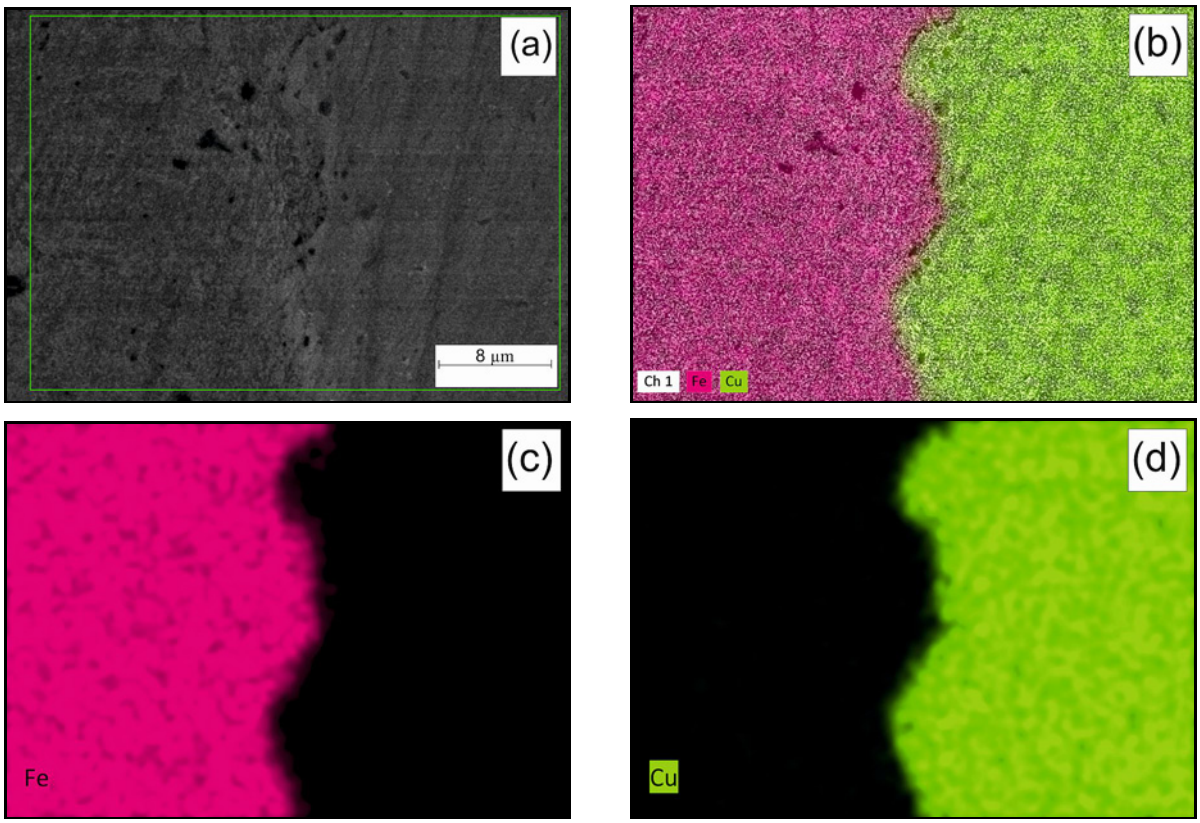

Fig. 7. Interface between steel core and copper layer: (a) with the corresponding EDS elemental mapping of Fe and Cu (b)–(d).

ular, the addition of other metals is, in most cases, too small to form significant amounts of carbides [9, 10]. The microstructure of the core of the Fe/Cu wire with a diameter of 1.50 mm after the patenting process consists of pearlite (Fig. 5). Pearlite consists of plates of ferrite and cementite formed by the breakdown of eutectoid austenite [11, 12]. The cementite plates are nanometric in size and are arranged in parallel in individual pearlitic colonies. The patenting process of the Fe/Cu bimetallic wire with a diameter of 1.50 mm is key to obtaining a wire with a final diameter of 0.20 mm without inter-operational heat treatment.

The interface between the steel core and the copper layer of the Fe/Cu wire was examined (Figs. 6, 7). Figure 6 shows a linear analysis of changes in the chemical composition of the Fe/Cu wire with a diameter of 1.50 mm after the wire patenting process. A good metallurgical bond between the steel core and the copper layer is visible. No intermetallic compounds were observed at the interface between the Fe core and the Cu layer, which could negatively affect the mechanical properties of the Fe/Cu wire and increase its electrical resistance [13]. The mapping performed at the interface between the steel core and the copper

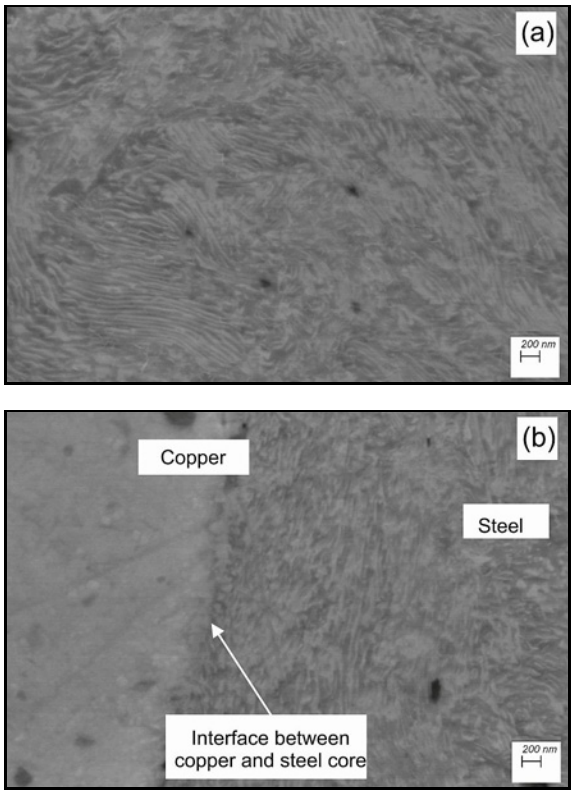

Fig. 8. Microstructure of the Fe/Cu wire with a diameter of 0.50 mm; cross-section, (a) steel core central zone and (b) Cu-Fe phase interface, SEM.

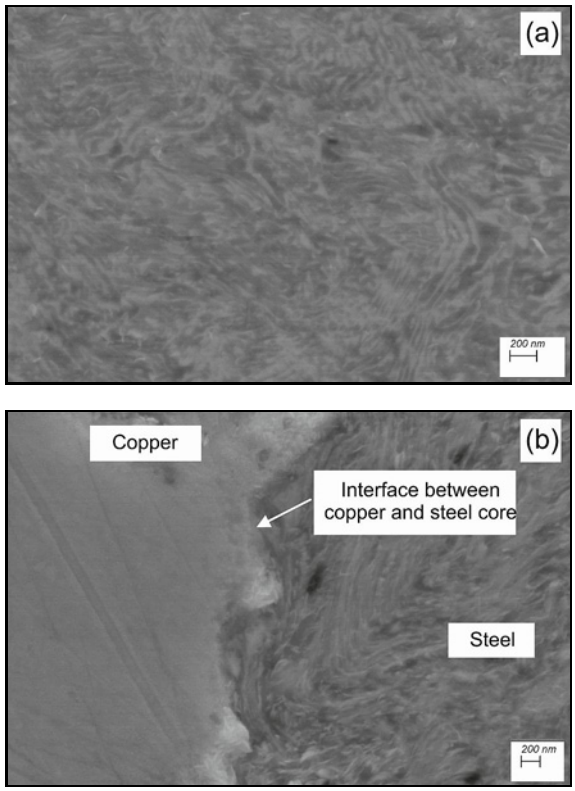

Fig. 9. Microstructure of the Fe/Cu wire with a diameter of 0.20 mm; cross-section: (a) steel core central zone and (b) Cu-Fe phase interface, SEM.

layer confirms a good metallurgical bonding.

Figures 8 and 9 show an example microstructure in cross-section of the Fe/Cu bimetallic wire core after cold drawing to a diameter of 0.50 and 0.20 mm. After subsequent drawing operations, the distance between the pearlite plates decreases. An increase in the degree of deformation causes fragmentation of the pearlite plates. It can be observed that individual pearlite colonies bend around the wire axis, which results from the reduction of the cross-sectional area of the wire. With increasing deformation, the pearlite plates become finer and resemble ribbons. Research conducted by the authors' team [9] using TEM reveals that adjacent ribbons have different orientations, which may result from many dislocations passing through the cementite from one ferrite sheet to the neighbouring one, with each dislocation slightly changing its orientation. Figures 8c and 9c show the interface between the copper layer and the steel core of the Fe/Cu wire with a diameter of 0.50 and 0.20 mm, respectively. A good metallurgical bonding between Fe and Cu is visible. There are no discontinuities in the final wire that could negatively affect the resistivity of these wires. A wavy shape of the boundary between the steel core and the copper layer is observed. No cracks, separations, or discontinuities are observed between Fe and Cu, indicating a strong bond between the steel core and the copper layer.

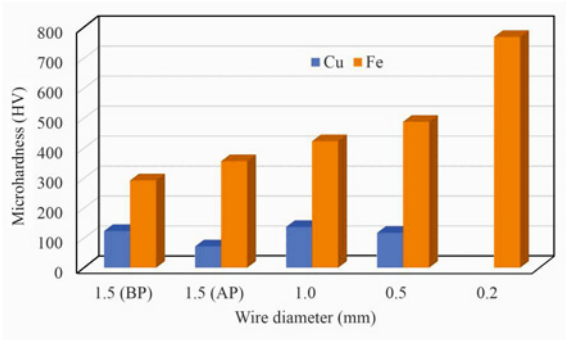

Fig. 10. Microhardness of the Fe/Cu bimetallic wire.

3.2. Mechanical properties

Figure 10 shows the average results of microhardness measurements taken on the cross-section of the Fe/Cu bimetallic wires with various degrees of total deformation. The average microhardness of the steel core of the Cu/Fe wire before patenting (BP) was 290 HV. As a result of the patenting process, the microhardness of the wire core increased to an average

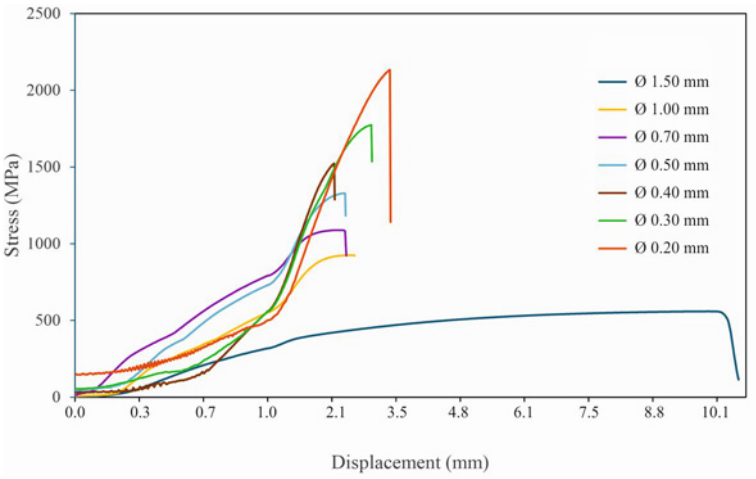

Fig. 11. The tensile test results of the Fe/Cu wire for different diameters (ø 1.50 mm wire after patenting).

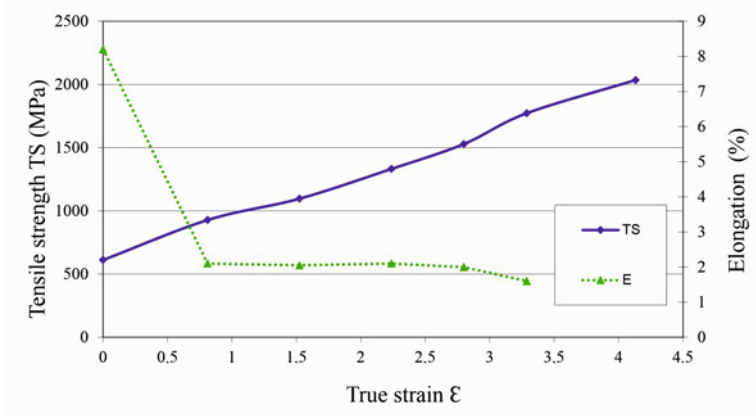

Fig. 12. Variation in tensile strength and elongation at the true strain.

value of 355 HV. As a result of deformation resulting from drawing the wire to the final diameter of 0.20 mm, the microhardness of the steel core of the wire increased to an average value of 770 HV. However, the hardened copper layer recrystallized after heat treatment of a 1.50 mm diameter wire, and as a result of subsequent deformation, the copper layer hardened. In the case of the Fe/Cu wire with a diameter of 0.20 mm, measuring the microhardness of the copper layer was impossible due to the copper layer being too thin – about 20 μm.

Figure 11 shows tensile curves (stress-displacement) of the Fe/Cu bimetallic wire for different diameters, i.e., 1.50 mm diameter wire after patenting, 1.0, 0.7, 0.5, 0.4, and 0.3 mm diameter wires, and the final 0.20 mm wire. Based on the static tensile test results, a strengthening curve was developed, which is particularly interesting for plastic processing technology. Figure 12 shows tensile strength (TS) and elongation (E) variation at the true strain. As shown, the Fe/Cu wire with a 1.50 mm diameter after the patenting process has the highest elongation and the lowest tensile strength. In subsequent drafts, the wire hardens, its tensile strength increases and with the final average diameter, it is approximately 2035 MPa. At the same time, the elongation of the wire decreases slightly.

During the tests of the mechanical properties of the wires at various stages of deformation, samples for fractographic tests on the occurred fractures were obtained. Based on the photos of the fractures, their nature was determined. Figure 13 illustrates the fractures obtained from a wire with a diameter of 1.50 mm after patenting and a diameter of 0.20 mm (300× magnification) along with the marked area of the steel core enlarged to 10,000× The observed fractures are plastic and fine-grained, which is particularly visible for the wire fracture with a diameter of 0.20 mm. As a result of breaking and tensile forces acting on the Fe/Cu wire with a diameter of 1.50 mm, a micro-gap becomes visible after patenting between the steel core of the wire and the copper layer.

3.3. Electrical properties

Figure 14 shows the electrical conductivity of the initial materials, i.e., copper and steel, and the final

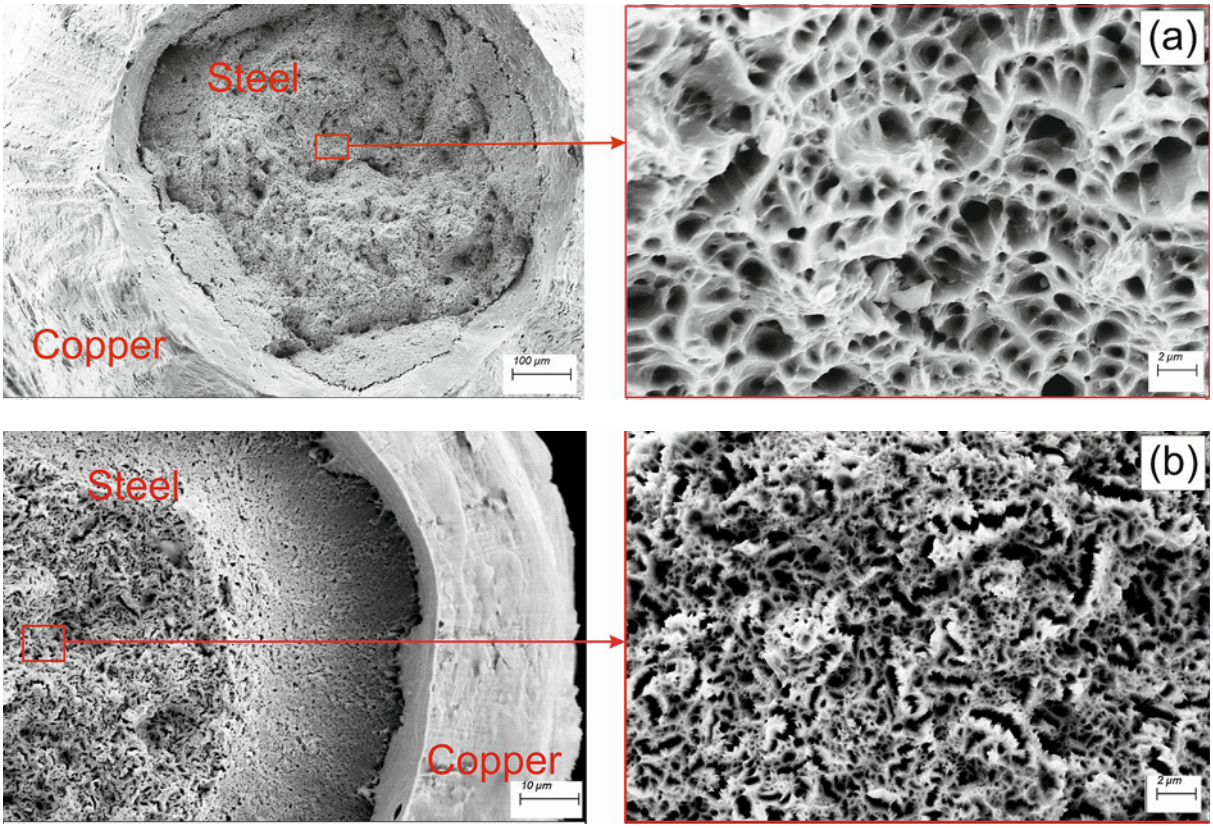

Fig. 13. SEM micrographs of the fracture surfaces of the wires drawn to fracture after cold-drawing (a) ø 1.50 mm and (b) ø 0.20 mm.

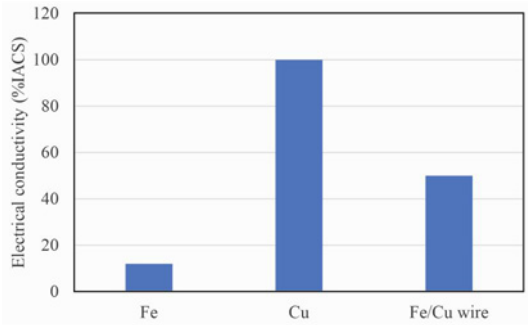

Fig. 14. Electrical properties of the initial materials and the final bimetallic Fe/Cu wire, ø 0.20 mm.

Fe/Cu bimetallic wire with a diameter of 0.20 mm. The share of the copper layer, approx. 50 % by volume ensured the high electrical conductivity of the Fe/Cu bimetallic wire at the level of approximately 50 % IACS.

4. Conclusions

The article presents the research results on the microstructure and mechanical and electrical properties of a Fe/Cu bimetallic wire produced using the rod-in-tube method. Based on the results obtained, the following conclusions were drawn:

1. The tests carried out in laboratory conditions allowed the production of a Fe/Cu bimetallic wire with a diameter of 0.20 mm with a copper share of approx. 50 % by volume, with high strength properties (approx. 2035 MPa) and high electrical conductivity (approx. 50 % IACS).

2. As a result of the patenting process of the Fe/Cu wire with a diameter of 1.50 mm, the steel core of the wire obtains a pearlitic structure, which allows drawing bimetallic wire up to a diameter of 0.20 mm without additional inter-operational heat treatment, with an average unit strain of 12 %.

3. The steel core obtains a full metallurgical bonding with the outer copper layer because of the large total deformation, 98 % of the bimetallic wire to a diameter of 0.20 mm.

4. Hard-drawn Fe/Cu wire combines the strength of steel with the conductivity of copper. These properties make this wire good for many telecommunications, utility, electronic and general industry applications.

Acknowledgement

This work was supported by subsidy funds of the

Łukasiewicz Research Network – Institute of Non-Ferrous Metals.

References

[1] W. Grünberger, M. Heilmaier, L. Schultz, High--strength, high-nitrogen stainless steel-copper composite wires for conductors in pulsed high-field magnets, Mater. Lett. 52 (2002) 154–158. https://doi.org/10.1016/S0167-577X(01)00383-4

[2] S. A. Nikulin, S. Rogachev, A. B. Rozhnov, V. I. Pantsyrnyi, N. E. Khlebova, T. A. Nechaykina, V. M. Khatkevich, M. Yu. Zadorozhnyy, Microstructure and fatigue strength of high-strength Cu–Fe and Cu–V in-situ nanocomposite wires, Composites B 70 (2015) 92–98. https://doi.org/10.1016/j.compositesb.2014.10.046

[3] F. Yang, X. Zang, F. Fang, Microstructure and properties of cold-drawn Cu and Cu-Fe alloy wires, IOP Conf. Ser.: Mater. Sci. Eng. 1249 (2022) 01205. https://doi.org/10.1088/1757-899X/1249/1/012057

[4] Y. Wang, Y. Gao, Y. Li, W. Zhai, L. Sun, C. Zhang, Review of preparation and application of copper–steel bimetal composites, Emerging Materials Research 8 (2019) 538–551. https://doi.org/10.1680/jemmr.17.00008

[5] S. Księżarek, W. Kazana, L. Ciura, K. Marszowski, M. Woch, Bimetallic wires: technology for their mechanical cold cladding and functional properties, Arch. Metall. Mater. 56 (2011) 891–895. https://doi.org/10.2478/v10172-011-0097-6

[6] W. Kazana, A. Płonka, M. Staszewski, Method of producing Fe-Cu bimetal wires, Patent PL224249, Institute of Non-Ferrous Metals in Gliwice, 2013.

[7] T. T. Sasaki, M. Barkley, G. B. Thompson, Y. Syarif, D. Fox, Microstructural evolution of copper clad steel bimetallic wire, Mater. Sci. Eng. 528 (2011) 2974–2981. https://doi.org/10.1016/j.msea.2010.12.032

[8] P. Ramkumar, F. Gino Prakash, M. K. Karthikeyan, R. K. Gupta, V. Muthupandi, Development of copper coating technology on high strength low alloy steel filler wire for aerospace applications, Materials Today: Proceedings 5 (2018) 7296–7302. https://doi.org/10.1016/j.matpr.2017.11.398

[9] Ch. Borchers, R. Kirchheim, Cold-drawn pearlitic steel wires, Prog. Mater. Sci. 82 (2016) 405–444. https://doi.org/10.1016/j.pmatsci.2016.06.001

[10] X. Zhang, A. Godfrey, X. Huang, N. Hansen, Q. Liu, Microstructure and strengthening mechanisms in cold--drawn pearlitic steel wire, Acta Materialia 59 (2011) 3422–3430. https://doi.org/10.1016/j.actamat.2011.02.017

[11] M. Zelin, Microstructure evolution in pearlitic steels during wire drawing, Acta Materialia 50 (2002) 4431–4447. https://doi.org/10.1016/S1359-6454(02)00281-1

[12] T.-Z. Zha, S.-H. Zhang, G.-L. Zhang, H.-W. Song, M. Cheng, Hardening and softening mechanisms of pearlitic steel wire under torsion, Materials and Design 59 (2014) 397–405. https://doi.org/10.1016/j.matdes.2014.03.029

[13] I.-K. Kim, S.-I. Hong, Mechanochemical joining in cold roll-cladding of tri-layered Cu/Al/Cu composite and the interface cracking behaviour, Materials and Design 57 (2014) 625–631. https://doi.org/10.1016/j.matdes.2014.01.054